Multipartite entanglement swapping and mechanical cluster states

Carlo Ottaviani,[1] Cosmo Lupo,[1] Alessandro Ferraro,[2] Mauro Paternostro,[2] and Stefano Pirandola[1,3]

[1]*Computer Science and York Centre for Quantum Technologies, University of York, York YO10 5GH, United Kingdom*

[2]*Centre for Theoretical Atomic, Molecular and Optical Physics, School of Mathematics and Physics, Queen's University Belfast, Belfast BT7 1NN, United Kingdom*

[3]*Research Laboratory of Electronics, Massachusetts Institute of Technology, Cambridge, Massachusetts 02139, USA*

We present a protocol for generating multipartite quantum correlations across a quantum network with a continuous-variable architecture. An arbitrary number of users possess two-mode entangled states, keeping one mode while sending the other to a central relay. Here a suitable multipartite detection is implemented, by multiple homodyne detections at the outputs of the interferometer, to conditionally generate a cluster state on the retained modes. This cluster state can be suitably manipulated by the parties and used for tasks of quantum communication in a fully optical scenario. More interestingly, the protocol can be used to create a purely-mechanical cluster state starting from a supply of optomechanical systems. We show that detecting the optical parts of optomechanical cavities may efficiently swap entanglement into their mechanical modes, creating cluster states up to five modes under suitable cryogenic conditions.

Introduction. Quantum teleportation [1–3] is one of the most important protocols in quantum information. Once two remote parties, say Alice and Bob, have distilled maximum entanglement, they can teleport quantum information with perfect fidelity from one location to another. In this kind of "disembodied" transport, the Bell detection [4,5] is one of the key operations. Connected with quantum teleportation is the teleportation of entanglement, also known as entanglement swapping [6–12]. Here, Alice and Bob start with two pairs of entangled states; they then send one part of each pair to a relay that performs Bell detection. This is a key mechanism for quantum repeaters [13–16], measurement-device independent quantum cryptography [17–22], as well as one of the tools of a future quantum internet [23,24].

In this work we introduce a multipartite entanglement swapping protocol for continuous-variable (CV) systems, such as optical and/or mechanical oscillators [25–29]. We consider an arbitrary number N of users, or "Bobs," each having the same identical two-mode Gaussian state ρ_{AB}. The B modes are kept, while the A modes are sent to a central relay performing multipartite Bell detection. The latter consists of an N-port interferometer, composed of $N-1$ cascaded beam splitters with suitable transmissivities, followed by N homodyne detections. The outcomes of homodyne detection are then publicly broadcast to all the users, which may locally apply conditional displacement operations.

The multipartite Bell detection is designed in such a way that the output multipartite state is a symmetric Gaussian state, i.e., invariant under the permutation of any two Bobs. In this way, we generate a type of Greenberger-Horne-Zeilinger (GHZ) cluster state that the Bobs may exploit for network tasks. In the literature, bosonic cluster states (also dubbed graph states) have been created with different procedures [25,30–34], typically via unitary processes, e.g., by applying

an interferometer to squeezed states [35,36]. Contrary to these schemes, our strategy fully extends the approach of Ref. [6] to a hybrid network [37,38], where a large supply of bipartite states with optomechanical entanglement are measured in the optical modes so that multipartite entanglement is swapped in the mechanical modes.

Following this idea, we present an application of the proposed protocol to the platform provided by cavity optomechanics [39], which has emerged in recent years as a promising route for the engineering of nonclassical features in mesoscopic systems. Various interesting schemes have been suggested and, in some cases, implemented with the scope of engineering quantum states of coupled optical and mechanical subsystems [40–45]. However, we lack a matching effort aimed at the preparation of nonclassical states of massive mechanical degrees of freedom [46–49]. In this respect, the protocol put forward here provides an interesting avenue toward the achievement of such a tantalizing goal.

Multipartite entanglement swapping. Consider an ensemble of $2N$ bosonic modes which are arranged into N pairs. We use the index $k = 1, \ldots, N$ for the pairs, and A, B for the modes within each pair (see Fig. 1). The whole system is described by a vector of quadratures

$$\xi = \left(X_1^A, P_1^A, X_1^B, P_1^B, \ldots, X_N^A, P_N^A, X_N^B, P_N^B \right)^T, \quad (1)$$

such that $[\xi_l, \xi_m] = 2i\mathbf{\Omega}_{lm}$, where $l, m = 1, \ldots, 2N$ and $\mathbf{\Omega}$ is the symplectic form [25]. Within each pair k, modes A and B are prepared in an entangled state ρ_{AB}. The A modes are sent to the interferometer depicted in Fig. 1, which is defined by $N-1$ beam splitters with transmissivities $T_k = 1 - k^{-1}$ for $k = 2, \ldots, N$. This interferometer transforms the input
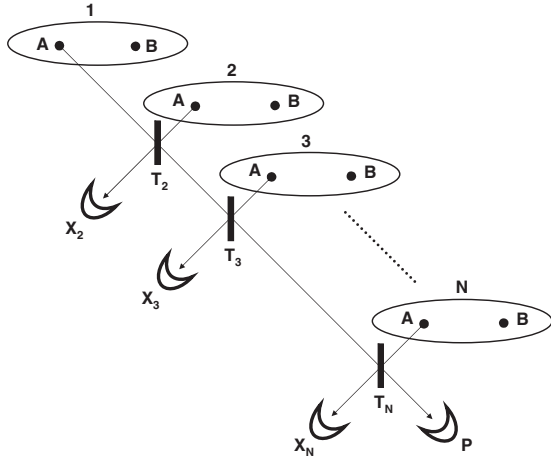
FIG. 1. Multipartite entanglement swapping. We start from N independent copies of the state ρ_{AB}. The A systems are sent to a relay for a multipartite CV Bell detection. The latter is an interferometer with a suitable cascade of beam splitters, followed by homodyne detections ($N - 1$ in the X quadratures, and a final one in the P quadrature). The outcomes γ are broadcast to the users, so that their multipartite state collapses into a conditional cluster state $\rho_{B_1 \cdots B_N | \gamma}$. The transmissivities T_k of the beam splitters are chosen so that the cluster state is invariant under permutation of the users.

quadratures into the output ones

$$X_k = \sqrt{1 - k^{-1}} \left(X_k^A - \frac{1}{k-1} \sum_{i=1}^{k-1} X_i^A \right), \qquad (2)$$

$$P = \frac{1}{\sqrt{N}} \sum_{k=1}^{N} P_k^A, \qquad (3)$$

which are then measured as in Fig. 1.

As a first example, consider N copies of an ideal Einstein-Podolsky-Rosen state, for which we may write [26]

$$P_k^A + P_k^B = 0, \quad X_k^A - X_k^B = 0, \qquad (4)$$

It is easy to show that the conditional state of the B modes is a multipartite CV version of the GHZ state [50], which satisfies the relations [26]

$$\sum_{k=1}^{N} P_k^B = 0, \qquad (5)$$

$$X_k^B - X_{k'}^B = 0, \quad \forall k, k' = 1, \dots, N. \qquad (6)$$

In fact, by projecting P in Eq. (3), we realize Eq. (5) up to a constant, which can be put to zero by a local displacement. In the same way, by projecting X_k in Eq. (2), we realize Eq. (6) up to constants [51].

Multiswapping of Gaussian states. Let us compute the cluster state generated by an input ensemble $\rho_{AB}^{\otimes N}$, where ρ_{AB} is a zero-mean Gaussian state with covariance matrix (CM) $\mathbf{V}$ in the normal form [52]

$$\mathbf{V} = \begin{pmatrix} x\mathbf{I} & z\mathbf{Z} \\ z\mathbf{Z} & y\mathbf{I} \end{pmatrix}, \qquad \mathbf{I} = \text{diag}(1, 1), \\ \mathbf{Z} = \text{diag}(1, -1). \qquad (7)$$

The computation of the CM of such N-mode conditional state, after the action of the interferometer, can be found in Ref. [53] (Supplemental Material). Here we give a brief summary. Consider a system of N pairs of bosonic modes, labeled A and B, with quadrature vector of the jth pair denoted $\xi_j = (X_j^A, P_j^A, X_j^B, P_j^B)^T$, for $j = 1, \dots, N$. In a symmetric setting all the pairs of modes are prepared in the same state of Eq. (7). To represent the system of $2N$ modes, we may define the quadrature vector as follows:

$$\xi = (\xi^A, \xi^B)^T$$
$$= \left(X_1^A, \dots, X_N^A, P_1^A, \dots, P_N^A, X_1^B, \dots, X_N^B, P_1^B, \dots, P_N^B \right)^T,$$

in terms of which the CM of the multimode can be written as

$$\mathbf{V} = \begin{pmatrix} x\mathbf{I}_N & 0 & z\mathbf{I}_N & 0 \\ 0 & x\mathbf{I}_N & 0 & -z\mathbf{I}_N \\ z\mathbf{I}_N & 0 & y\mathbf{I}_N & 0 \\ 0 & -z\mathbf{I}_N & 0 & y\mathbf{I}_N \end{pmatrix}, \qquad (8)$$

where I_N denotes the $N \times N$ identity matrix. Noticing that the evolution of the input state through the interferometer and the local homodyne detections on the A modes commute, as long as the input state has the form of Eq. (8), we can first apply the local homodynes and then evolve the resulting state through the interferometer. After the multipartite Bell detection of modes A and the broadcast of the outcome γ, the conditional cluster state $\rho_{B_1 \cdots B_N | \gamma}$ of the B modes is a symmetric Gaussian state, described by the following CM:

$$\mathbf{V}_{B_1 \cdots B_N | \gamma} = \begin{pmatrix} \mathbf{V}' & \mathbf{C}' & \cdots & \mathbf{C}' \\ \mathbf{C}' & \mathbf{V}' & & \vdots \\ \vdots & & \ddots & \mathbf{C}' \\ \mathbf{C}' & \cdots & \mathbf{C}' & \mathbf{V}' \end{pmatrix}, \qquad (9)$$

where the blocks are given by

$$\mathbf{V}' = \begin{pmatrix} y - \frac{N-1}{N}\frac{z^2}{x} & 0 \\ 0 & y - \frac{z^2}{Nx} \end{pmatrix}, \quad \mathbf{C}' = \frac{z^2}{Nx}\mathbf{Z}. \qquad (10)$$

Using Eq. (9), we may connect the log negativity [27] $E_{\mathcal{N}}^{(N)}$ between any two Bobs, B_i and B_j, with the log negativity $E_{\mathcal{N}}^{\text{in}}$ of the input state ρ_{AB}. For $N = 2$ we may show a quasi-monotonic relation as in Fig. 2(a), where the gray region is generated by randomly sampling the input CM of Eq. (7) with a known parametrization [54]. The upper bound is achieved by two-mode squeezed vacuum (TMSV) states, while the lower bound corresponds to states with large asymmetry parameter $d := (x - y)/2$. The detrimental role of the asymmetries can also be appreciated in Fig. 2(b), where $E_{\mathcal{N}}^{(2)}$ is plotted versus d.

Cluster states in optical networks. In applications of quantum communication, the users may be located remotely so as to access the Bell detection via lossy optical links. Because of the fundamental limitations affecting these links [55], the cluster state is also degraded by loss and noise. Assume that each Bob has a TMSV state with variance $\mu \geqslant 1$ [25]. After propagating the A mode through a thermal-loss channel with transmissivity η and thermal noise ω, the input state ρ_{AB} has CM as in Eq. (7) with $x = \eta\mu + (1 - \eta)\omega$, $y = \mu$, and $z = \sqrt{\eta}\sqrt{\mu^2 - 1}$.
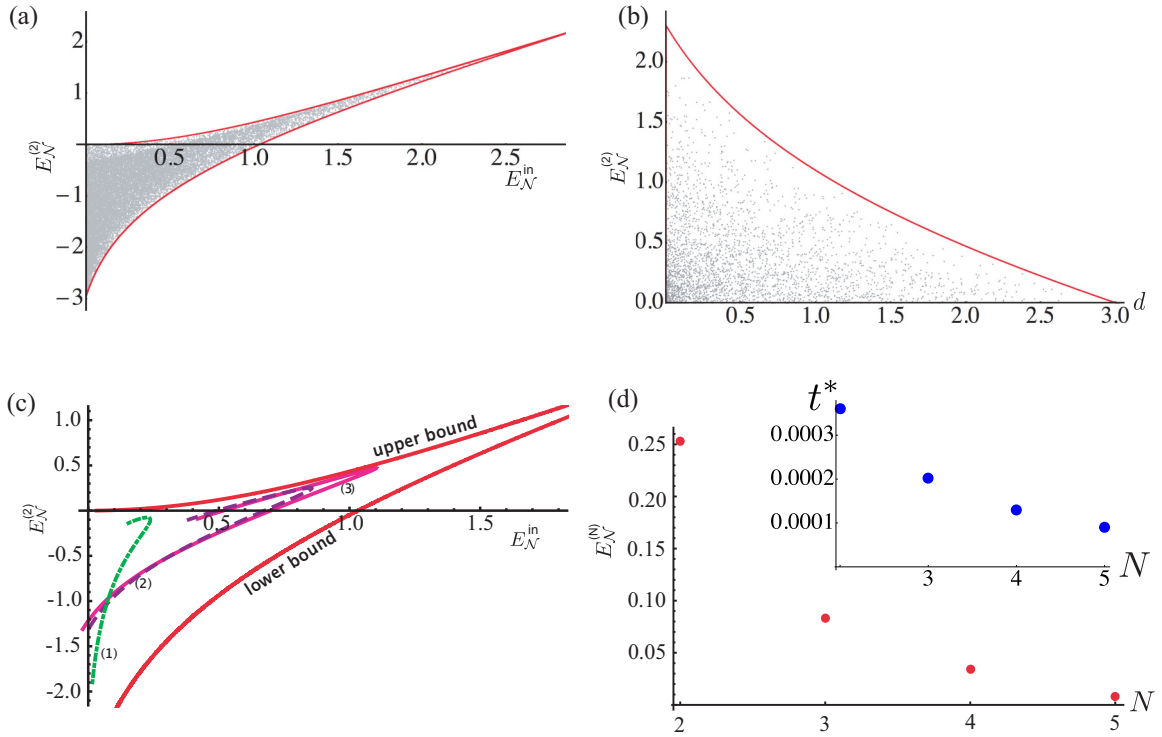
FIG. 2. Study of the output mechanical entanglement. (a) For $N = 2$ we plot the output log negativity $E_{\mathcal{N}}^{(2)}$ as a function of the log negativity $E_{\mathcal{N}}^{\text{in}}$ of the input Gaussian state which is generated by random sampling. Upper and lower bounds (solid lines) are achieved by the classes of states discussed in the main text. (b) We show the distribution of $E_{\mathcal{N}}^{(2)}$ as a function of the asymmetry parameter d by randomly sampling the input state. The solid line shows the maximum achievable value. (c) We plot the output log negativity $E_{\mathcal{N}}^{(2)}$ of two mechanical modes as a function of the input log negativity $E_{\mathcal{N}}^{\text{in}}$ between the optical and the mechanical modes of two identical optomechanical systems with parameters $\gamma_m/2\pi = 100$ Hz, $\omega_m/2\pi = 10$ MHz, $\kappa/2\pi = 31.4$ MHz, and $T = 0.4$ mK. Each mechanical mode has mass $m = 5$ ng. The green dashed line (1), the dashed purple (2), and the solid magenta (3), correspond to effective optomechanical coupling rates of $2\pi \times 4$ MHz, $2\pi \times 8$ MHz, and $2\pi \times 8.5$ MHz, respectively. These values match closely those typical of a photonic-crystal-based optomechanical architecture [63]. The curvilinear abscissa of each line is the detuning $\Delta \in [0, 1.5\omega_m]$. (d) We show the output log negativity $E_{\mathcal{N}}^{(N)}$ between any two modes in a cluster of N mechanical modes, for $N = 2$–5. Parameters as in panel (c) with an effective optomechanical coupling strength of $2\pi \times 8$ MHz. Inset: we show the time t^* (s) at which the entanglement $E_{\mathcal{N}}^{(N)}$ disappears when assuming dissipation into independent thermal baths at temperature T for each involved mechanical mode.

From Eq. (9) we can compute the corresponding N-user symmetric cluster state that is generated by the multipartite Bell detection. From the N-partite system of Eq. (9), we consider the bipartite case where $N = 2$. We write the CM of a bipartite in the following general form:

$$\tilde{\mathbf{V}} = \begin{pmatrix} a & 0 & c & 0 \\ 0 & b & 0 & c' \\ c & 0 & a & 0 \\ 0 & c' & 0 & b \end{pmatrix}, \tag{11}$$

from which we compute the log negativity, defined as

$$E_{\mathcal{N}} = \max\{0, -\ln \nu_-\}, \tag{12}$$

where ν_- is the smallest symplectic eigenvalue of the partially transposed CM obtained from $\tilde{\mathbf{V}}$ applying the following transformation:

$$\mathbf{V}^{PT} = \mathbf{\Lambda} \tilde{\mathbf{V}} \mathbf{\Lambda}, \tag{13}$$

where diagonal matrix $\mathbf{\Lambda} := \text{diag}[1, 1, 1, -1]$. The symplectic spectrum is obtained diagonalizing matrix $\mathbf{M} = |i\mathbf{\Omega} \mathbf{V}^{PT}|$

[25], from which one has

$$\nu_- = \sqrt{(a - c)(b + c')}, \quad \nu_+ = \sqrt{(a + c)(b - c')}. \tag{14}$$

Setting $a = y - \frac{z^2}{2x} = b$, and $c' = -\frac{z^2}{2x} = -c$ in Eq. (11), ν_- takes the form

$$\nu_- = \sqrt{\left(y - \frac{z^2}{x}\right)\left(y - \frac{z^2}{x}\right)} = y - \frac{z^2}{x}. \tag{15}$$

From the expression of $x = \eta\mu + (1 - \eta)\omega$, $y = \mu$, $z = \sqrt{\eta(\mu^2 - 1)}$, and using the definition of Eq. (12), we obtain the log negativity of the bipartite system

$$E_{\mathcal{N}}^{(2)} = \ln \frac{\eta\mu + (1 - \eta)\omega}{\eta + (1 - \eta)\mu\omega}. \tag{16}$$

Now, consider an arbitrary block of the general multipartite state of Eq. (9), describing a reduced bipartite system. The smallest symplectic eigenvalue is given by

$$\nu_-^{(N)} = \sqrt{\left(y - \frac{z^2}{x}\right)\left(y - \frac{2z^2}{Nx}\right)}. \tag{17}$$

From this one can write

$$\nu_-^{(N)} = \sqrt{\left(y - \frac{z^2}{x}\right)\left(y - \frac{z^2}{x} + \frac{z^2}{x} - \frac{2z^2}{Nx}\right)},$$

$$= \left(y - \frac{z^2}{x}\right)\sqrt{1 + \frac{N-2}{N}\frac{\eta(\mu^2 - 1)}{\eta + (1-\eta)\mu\omega}}$$

$$= \left(y - \frac{z^2}{x}\right)\sqrt{1 + \frac{N-2}{N}\alpha}, \tag{18}$$

where $\alpha := \eta(\mu^2 - 1)[\eta + (1-\eta)\mu\omega]^{-1}$. Using the definition of Eqs. (12), (15), and (16), one finds that the log negativity $E_{\mathcal{N}}^{(N)}$ between any pair of Bobs is given by

$$E_{\mathcal{N}}^{(N)} = E_{\mathcal{N}}^{(2)} - \frac{1}{2}\ln\left(1 + \alpha\frac{N-2}{N}\right), \tag{19}$$

where $\alpha := \eta(\mu^2 - 1)[\eta + (1-\eta)\mu\omega]^{-1}$. The presence of α in Eq. (19) shows that loss η and noise ω destroy entanglement more rapidly as N increases [56].

Once the cluster state has been generated, the users may also cooperate in such a way to concentrate the multipartite entanglement into more robust bipartite forms. For instance, they may localize the entanglement into a pair of users by means of quantum operations performed by all the others [57]. If these operations are Gaussian, this is called Gaussian localizable entanglement (GLE) [58,59]. In such a case, the entanglement between two arbitrary subsets A and B of users, with cardinality N_A and N_B, such that $N_A + N_B \leqslant N$, is equivalent to the entanglement between two modes described by the following CM:

$$V_{AB} = \begin{pmatrix} \gamma_A & 0 & \delta & 0 \\ 0 & \bar{\gamma}_A & 0 & -\delta \\ \delta & 0 & \gamma_B & 0 \\ 0 & -\delta & 0 & \bar{\gamma}_B \end{pmatrix}, \tag{20}$$

where $\gamma_A = y - \frac{N-N_A}{N}\frac{z^2}{x}$, $\bar{\gamma}_A = y - \frac{N_A}{N}\frac{z^2}{x}$, $\gamma_B = y - \frac{N-N_B}{N}\frac{z^2}{x}$, $\bar{\gamma}_B = y - \frac{N_B}{N}\frac{z^2}{x}$, and $\delta = \frac{\sqrt{N_A N_B}}{N}\frac{z^2}{x}$.

The localizable entanglement is defined as the maximum entanglement (quantified by a suitable entanglement measure) that can be localized between a given pair of users by optimizing operations on the other $N-2$ users. By applying a unitary transformation on $N-2$ users, our state can always be reduced to a three-mode Gaussian state with CM [58]

$$V_{\text{loc}} = \begin{pmatrix} \Delta & 0 & \epsilon & 0 & \epsilon' & 0 \\ 0 & \Delta' & 0 & -\epsilon & 0 & -\epsilon' \\ \epsilon & 0 & \Delta & 0 & \epsilon' & 0 \\ 0 & -\epsilon & 0 & \Delta' & 0 & -\epsilon' \\ \epsilon' & 0 & \epsilon' & 0 & \Phi & 0 \\ 0 & -\epsilon' & 0 & -\epsilon' & 0 & \Phi' \end{pmatrix}, \tag{21}$$

where $\Delta = y - \frac{N-1}{N}\frac{z^2}{x}$, $\Delta' = y - \frac{1}{N}\frac{z^2}{x}$, $\Phi = y - \frac{2}{N}\frac{z^2}{x}$, $\Phi' = y - \frac{N-2}{N}\frac{z^2}{x}$, $\epsilon = \frac{1}{N}\frac{z^2}{x}$, and $\epsilon' = \frac{\sqrt{N-2}}{N}\frac{z^2}{x}$. Since the original state is symmetric under the permutation of the users, the results of Ref. [59] imply that homodyne detection on the third mode is optimal (among Gaussian measurements) to maximize the logarithmic negativity between the first pair of modes. We find that the GLE log negativity between any pair

of Bobs in the N-user cluster state is

$$E_{\mathcal{N}}^{(N,\text{GLE})} = E_{\mathcal{N}}^{(2)} - \frac{1}{2}\ln\left(1 + \frac{N-2}{\alpha^{-1}N + 2}\right). \tag{22}$$

Suppose instead that the Bobs split into two groups of N' users, so that $2N' \leqslant N$. Passive unitary operations within the two groups may map the state into a tensor product of $2N - 2$ uncorrelated single-mode states and one correlated two-mode state [60]. The log negativity of the block entanglement associated with the symmetric splitting (N', N') of the Bobs is given by

$$E_{\mathcal{N}}^{(N,N')} = E_{\mathcal{N}}^{(2)} - \frac{1}{2}\ln\left(1 + \alpha\frac{N-2N'}{N}\right). \tag{23}$$

Note that this is just equal to $E_{\mathcal{N}}^{(2)}$ for the "full-house" splitting $N' = N/2$. This is a robust concentration of entanglement because it no longer depends on N.

Generation of mechanical cluster states. We now consider the generation of a mechanical cluster state by applying the multipartite Bell detection to the optical parts of N optomechanical systems. More precisely, consider N systems embodied by single-sided Fabry-Perot optomechanical cavities, driven by external laser fields of suitable intensity. The mechanical systems embody modes B_k, while the corresponding cavity fields are the A_k's. In a reference frame rotating at the frequency of the input driving field, each A_k-B_k interaction is modeled through the standard radiation-pressure Hamiltonian

$$\hat{H}_k = \hbar\Delta\hat{a}_k^\dagger\hat{a}_k + \frac{\hbar\omega_m}{2}(\hat{q}_k^2 + \hat{p}_k^2)$$
$$- \hbar G_0\hat{a}_k^\dagger\hat{a}_k\hat{q} + iE\hbar(\hat{a}_k^\dagger - \hat{a}_k). \tag{24}$$

Here, $\hat{q}_k$ and $\hat{p}_k$ are the dimensionless quadrature operators of the kth mechanical system, $\hat{a}_k$ and $\hat{a}_k^\dagger$ are the ladder operators of the corresponding cavity field, ω_m is the frequency of the mechanical mode (assumed to be the same for all the mechanical systems), G_0 is the optomechanical coupling rate, and E is the amplitude of the laser drive. Finally, Δ is the laser-driven cavity detuning.

The dynamics resulting from the Hamiltonian $\hat{H}_k$ is affected by the cavity energy decay (at a rate κ) and the Brownian motion of the mechanical oscillator (induced by the contact of each mechanical system with a background of phonons in thermal equilibrium at temperature T), characterized by the coupling strength γ_m. The mechanical system is thus assumed to be prepared, prior to the optomechanical interaction, in a thermal state at temperature T. The cavity is instead in a coherent state with amplitude determined by the choice of E and κ [61,62].

Under such conditions, the open dynamics at hand is well described by a set of Langevin equations obtained considering the fluctuations around the mean values of the operators in the problem and neglecting any nonlinearity. This is a well-established technique allowing for the gathering of information on the quantum statistical properties of the system, as far as the fluctuations of the operators are small compared to the mean values. References [61,62] provide the details of the formal approach and steps to take to derive the explicit form of the CM of the kth optomechanical system. From this point on,

our proposed protocol for multipartite entanglement swapping can be applied as per the previous sections.

The results are shown in Fig. 2(c) for the case of $N = 2$ and three different choices of parameters in the optomechanical building block. The first consideration to make is that, in line with the analysis of random Gaussian states previously reported, the symmetry between modes A_k and B_k facilitates the success of the protocol: our numerical study shows that only for $T \ll 1$, which makes the variances associated with the fluctuation operators of the mechanical mode close to those of the cavity field, all-mechanical entanglement might arise from the application of the protocol. Second, such entanglement benefits of a suitably strong optomechanical coupling rate, resulting in values that can approach the upper boundary to the distribution in Fig. 2(a). The parameters used for the simulation reported in Fig. 2(c) are close to those currently available in photonic-crystal-based optomechanical platform, where acoustic modes ranging from a few megahertz to a few gigahertz and couplings in the 10 MHz range are available for $\kappa \simeq 50$ MHz [63].

Our results demonstrate the effectiveness of the proposed scheme as a method for the achievement of all-mechanical entanglement through optical measurements only. However, the significance of the scheme goes beyond such a fundamental result and extends to the potential preparation of multipartite entangled mechanical states. Indeed, we have verified that the protocol remains successful when applied to systems of up to $N = 5$ optomechanical building blocks, as shown in Fig. 2(d), where we report the value of the maximum entanglement achieved as N grows from 2 to 5, for the most realistic choice of the effective optomechanical coupling strength. By assuming that, following the preparation of the mechanical cluster state, each mechanical mode is subjected to dissipation into individual baths at temperature T, it is possible to show that such entanglement persists within the engineered multipartite state for a time that depends on the number of particles involved in the protocol. The inset of Fig. 2(d) shows the time at which $E_{\mathcal{N}}^N$ disappears. Such times allow for $\simeq 100$ coherent operations on the mechanical system at the optomechanical coupling rate assumed in Fig. 2(d).

Conclusions. We have introduced a protocol of multipartite entanglement swapping for CV systems, based on a multipartite version of the standard CV Bell detection. We have studied how this protocol is able to generate an entangled cluster state in an optical lossy network, whose entanglement can be suitably manipulated and localized by the users. Such multipartite CV entangled states are useful for tasks of quantum communication, cluster-state quantum computation [25], multiuser quantum cryptography, and distributed quantum sensing.

We have then proposed a powerful implementation of our protocol that exploits an optomechanical interface designed to efficiently transfer entanglement onto the mechanical modes of N optomechanical cavities. Our results pave the way toward applications for quantum technologies and networking with hybrid architecture providing a potentially fruitful alternative to recent experimental demonstrations of all-mechanical entanglement [64,65].

[1] C. H. Bennett, G. Brassard, C. Crepeau, R. Jozsa, A. Peres, and W. K. Wootters, Phys. Rev. Lett. **70**, 1895 (1993).

[2] S. L. Braunstein and H. J. Kimble, Phys. Rev. Lett. **80**, 869 (1998).

[3] S. Pirandola, J. Eisert, C. Weedbrook, A. Furusawa, and S. L. Braunstein, Nat. Photonics **9**, 641 (2015).

[4] H. Weinfurter, Europhys. Lett. **25**, 559 (1994).

[5] S. L. Braunstein and A. Mann, Phys. Rev. A **51**, R1727 (1995).

[6] S. Pirandola, D. Vitali, P. Tombesi, and S. Lloyd, Phys. Rev. Lett. **97**, 150403 (2006).

[7] M. Żukowski, A. Zeilinger, M. A. Horne, and A. K. Ekert, Phys. Rev. Lett. **71**, 4287 (1993).

[8] P. van Loock and S. L. Braunstein, Phys. Rev. A **61**, 010302(R) (1999).

[9] R. E. S. Polkinghorne and T. C. Ralph, Phys. Rev. Lett. **83**, 2095 (1999).

[10] S. Bose, V. Vedral, and P. L. Knight, Phys. Rev. A **57**, 822 (1998).

[11] A. M. Goebel, C. Wagenknecht, Q. Zhang, Y.-A. Chen, K. Chen, J. Schmiedmayer, and J.-W. Pan, Phys. Rev. Lett. **101**, 080403 (2008).

[12] C.-Y. Lu, T. Yang, and J.-W. Pan, Phys. Rev. Lett. **103**, 020501 (2009).

[13] H.-J. Briegel, W. Dür, J. I. Cirac, and P. Zoller, Phys. Rev. Lett. **81**, 5932 (1998).

[14] W. Dür, H.-J. Briegel, J. I. Cirac, and P. Zoller, Phys. Rev. A **59**, 169 (1999).

[15] L. M. Duan, M. D. Lukin, J. I. Cirac, and P. Zoller, Nature (London) **414**, 413 (2001).

[16] S. Pirandola, arXiv:1601.00966.

[17] S. L. Braunstein and S. Pirandola, Phys. Rev. Lett. **108**, 130502 (2012).

[18] H.-K. Lo, M. Curty, and B. Qi, Phys. Rev. Lett. **108**, 130503 (2012).

[19] S. Pirandola, C. Ottaviani, G. Spedalieri, C. Weedbrook, S. L. Braunstein, S. Lloyd, T. Ghering, C. S. Jacobsen, and U. L. Andersen, Nat. Photonics **9**, 397 (2015).

[20] S. Pirandola, C. Ottaviani, G. Spedalieri, C. Weedbrook, S. L. Braunstein, S. Lloyd, T. Ghering, C. S. Jacobsen, and U. L. Andersen, Nat. Photonics **9**, 773 (2015).

[21] C. Ottaviani, G. Spedalieri, S. L. Braunstein, and S. Pirandola, Phys. Rev. A **91**, 022320 (2015).

[22] P. Papanastasiou, C. Ottaviani, and S. Pirandola, Phys. Rev. A **96**, 042332 (2017).

[23] H. J. Kimble, Nature (London) **453**, 1023 (2008).

[24] S. Pirandola and S. L. Braunstein, Nature (London) **532**, 169 (2016).

[25] C. Weedbrook, S. Pirandola, R. García-Patrón, N. J. Cerf, T. C. Ralph, J. H. Shapiro, and S. Lloyd, Rev. Mod. Phys. **84**, 621 (2012).

[26] S. L. Braunstein and P. van Loock, Rev. Mod. Phys. **77**, 513 (2005).

[27] A. Ferraro, S. Olivares, and M. G. A. Paris, *Gaussian States in Quantum Information* (Bibliopolis, Napoli, 2005).

[28] G. Adesso, S. Ragy, and A. R. Lee, Open Syst. Inf. Dyn. **21**, 1440001 (2014).

[29] A. Serafini, *Quantum Continuous Variables: A Primer of Theoretical Methods* (Taylor & Francis, Oxford, 2017).

[30] D. Gross and J. Eisert, Phys. Rev. Lett. **98**, 220503 (2007).

[31] M. A. Nielsen, Phys. Rev. Lett. **93**, 040503 (2004).

[32] N. C. Menicucci, P. van Loock, M. Gu, C. Weedbrook, T. C. Ralph, and M. A. Nielsen, Phys. Rev. Lett. **97**, 110501 (2006).

[33] J. Zhang and S. L. Braunstein, Phys. Rev. A **73**, 032318 (2006).

[34] S. Yokoyama, R. Ukai, S. C. Armstrong, C. Sornphiphatphong, T. Kaji, S. Suzuki, J. Yoshikawa, H. Yonezawa, N. C. Menicucci, and A. Furusawa, Nat. Photon. **7**, 982 (2013).

[35] P. van Loock and S. L. Braunstein, Phys. Rev. Lett. **84**, 3482 (2000).

[36] H. Yonezawa, T. Aoki, and A. Furusawa, Nature (London) **431**, 430 (2004).

[37] U. L. Andersen, J. S. Neergaard-Nielsen, P. van Loock, and A. Furusawa, Nat. Phys. **11**, 713 (2015)

[38] G. Kurizki *et al.*, Proc. Natl. Acad. Sci. U.S.A. **112**, 3866 (2015).

[39] M. Aspelmeyer, T. J. Kippenberg, and F. Marquardt, Rev. Mod. Phys. **86**, 1391 (2014).

[40] T. A. Palomaki, J. D. Teufel, R. W. Simmonds, and K. W. Lehnert, Science **342**, 710 (2013).

[41] R. Riedinger, S. Hong, R. A. Norte, J. A. Slater, J. Shang, A. G. Krause, V. Anant, M. Aspelmeyer, and S. Gröblacher, Nature (London) **530**, 313 (2016).

[42] T. Palomaki, J. Harlow, J. Teufel, R. Simmonds, and K. Lehnert, Nature (London) **495**, 210 (2013).

[43] D. W. Brooks, T. Botter, S. Schreppler, T. P. Purdy, N. Brahms, and D. M. Stamper-Kurn, Nature (London) **488**, 476 (2012).

[44] T. P. Purdy, P.-L. Yu, R. W. Peterson, N. S. Kampel, and C. A. Regal, Phys. Rev. X **3**, 031012 (2013).

[45] A. H. Safavi-Naeini, S. Gröblacher, J. T. Hill, J. Chan, M. Aspelmeyer, and O. Painter, Nature (London) **500**, 185 (2013).

[46] D. Vitali, S. Mancini, and P. Tombesi, J. Phys. A: Math. Theor. **40**, 8055 (2007).

[47] M. Abdi, S. Pirandola, P. Tombesi, and D. Vitali, Phys. Rev. Lett. **109**, 143601 (2012).

[48] M. Abdi, S. Pirandola, P. Tombesi, and D. Vitali, Phys. Rev. A **89**, 022331 (2014).

[49] O. Houhou, H. Aissaoui, and A. Ferraro, Phys. Rev. A **92**, 063843 (2015).

[50] D. M. Greenberger, M. A. Horne, and A. Zeilinger, in *Bell's Theorem, Quantum Theory, and Conceptions of the Universe*, edited by M. Kafatos (Kluwer Academic, Dordrecht, 1989), pp. 73–76.

[51] In fact, according to Eqs. (2) and (3), the first projection onto X_2 gives (up to a constant) $X_1^A - X_2^A = 0$. By using the latter in the expression of X_3, we derive $\sqrt{6}X_3 = 2X_1^A - 2X_3^A$. The projection onto X_3 gives therefore the second condition $X_1^A - X_3^A = 0$, and so on.

[52] S. Pirandola, A. Serafini, and S. Lloyd, Phys. Rev. A **79**, 052327 (2009).

[53] C. Ottaviani, C. Lupo, R. Laurenza, and S. Pirandola, arXiv:1709.06988.

[54] G. Adesso and F. Illuminati, Phys. Rev. A **72**, 032334 (2005).

[55] S. Pirandola, R. Laurenza, C. Ottaviani, and L. Banchi, Nat. Commun. **8**, 15043 (2017).

[56] In lossless and noiseless conditions ($\eta = \omega = 1$), for large μ we may write $E_\mathcal{N}^{(N)} = -\frac{1}{2}\ln(1 - 2/N)$, which is always positive but scales as $O(1/N)$.

[57] M. Popp, F. Verstraete, M. A. Martín-Delgado, and J. I. Cirac, Phys. Rev. A **71**, 042306 (2005).

[58] J. Fiurasek, and L. Mista, Jr., Phys. Rev. A **75**, 060302(R) (2007).

[59] L. Mišta, Jr. and J. Fiurášek, Phys. Rev. A **78**, 012359 (2008).

[60] A. Serafini, G. Adesso, and F. Illuminati, Phys. Rev. A **71**, 032349 (2005).

[61] M. Paternostro *et al.*, New J. Phys. **8**, 107 (2006).

[62] D. Vitali, S. Gigan, A. Ferreira, H. R. Böhm, P. Tombesi, A. Guerreiro, V. Vedral, A. Zeilinger, and M. Aspelmeyer, Phys. Rev. Lett. **98**, 030405 (2007).

[63] M. Kalaee, T. K. Paraïso, H. Pfeifer, and O. Painter, Opt. Express **24**, 21308 (2016).

[64] R. Riedinger, A. Wallucks, I. Marinkovic, C. Löschnauer, M. Aspelmeyer, S. Hong, and S. Gröblacher, Nature **556**, 473 (2018).

[65] C. F. Ockeloen-Korppi, E. Damskagg, J.-M. Pirkkalainen, A. A. Clerk, F. Massel, M. J. Woolley, and M. A. Sillanpaa, Nature (London) **556**, 478 (2018).